Supplement of

Characterization of NR-PM$_1$ and source apportionment of organic aerosol in Krakow, Poland

Anna K. Tobler et al.
Correspondence to: A.S.H. Prévôt (andre.prevot@psi.ch)

S1 Quality control of Aethalometer eBC measurements

The eBC mass concentration measured with Aethalometers was calibrated as the relationship between the optical measurement of light attenuation (ATN) and the thermal measurement of carbonaceous mass on filters extracted of non-refractive material (Gundel et al., 1984). The slope of this relationship is the mass attenuation cross-section. Gundel et al. (1984) used urban samples for their calibration. The ratio between the mass attenuation cross-section and MAC is the multiple scattering enhancement parameter C, the multiplication parameter describing the light absorption enhancement due to the light scattering filter matrix in which the particles are embedded (Drinovec et al., 2015). The eBC measurement is cross-sensitive to scattering (Drinovec et al., 2015) with the susceptibility depending on the filter type and the sample (Yus et al., 2021). These site-dependent artifacts are explicitly observed as the changes in the slope between different filter photometers in regional background sites, featuring high single-scattering albedo (Zanatta et al., 2016; Yus et al., 2021).

The continuity of calibration of Aethalometers was ensured with comparisons at urban sites with low single-scattering albedo and fresh aerosol (Gundel et al., 1984; Drinovec et al., 2015). The measurement artifacts related to high single-scattering albedo, internal mixing of aged BC and cross-sensitivity to scattering are not prevalent in urban atmospheres (Yus et al., 2021) and therefore we do not expect them to be relevant for our studies in Krakow. The eBC mass concentration should be linearly dependent on the time derivative of ATN, there should be no dependence on ATN itself – any dependence is the manifestation of the loading non-linearities of the measurement, that is the saturation of the measurement and the associated decrease of measurement the sensitivity.

In Fig. S1 we see the BC(ATN) plot determined from the data for the whole measurement campaign from January 2018 to April 2019, for the wavelengths used in the source apportionment algorithm (Sandradewi et al., 2008): 470 nm and 950 nm. The slope, remaining after the internal correction by the Aethalometer (Drinovec et al., 2015), is minimal with the artifact below 5% for the case of 950 nm channel and even less for the 470 nm channel.

The maximum ATN at which the measurements are restarted on a new piece of tape (tape is advanced) is set for UV as ATN_{max} (370 nm) =120. This translates to ATN_{max} (950 nm) = 46, assuming BC is the only component of the sample and this parameter changes inversely with wavelength – this is the same assumption as taking absorption Angstrom exponent AAE=1. The real value at 950 nm depends on the real sample absorption at this wavelength of interest, therefore on the wavelength dependence of absorption and hence AAE. So, the value at 950 nm is lower than what one would expect by assuming AAE=1 and extrapolating from 370nm. Additionally, high concentrations with very loaded filter (high ATN) trigger the advance of tape and start of the measurement with a fresh tape (ATN = 0). To void the bias due to these very high concentrations, we have determined the slope in the interval between ATN=2 and ATN = 0.85 ATN_{max} for each wavelength of interest.

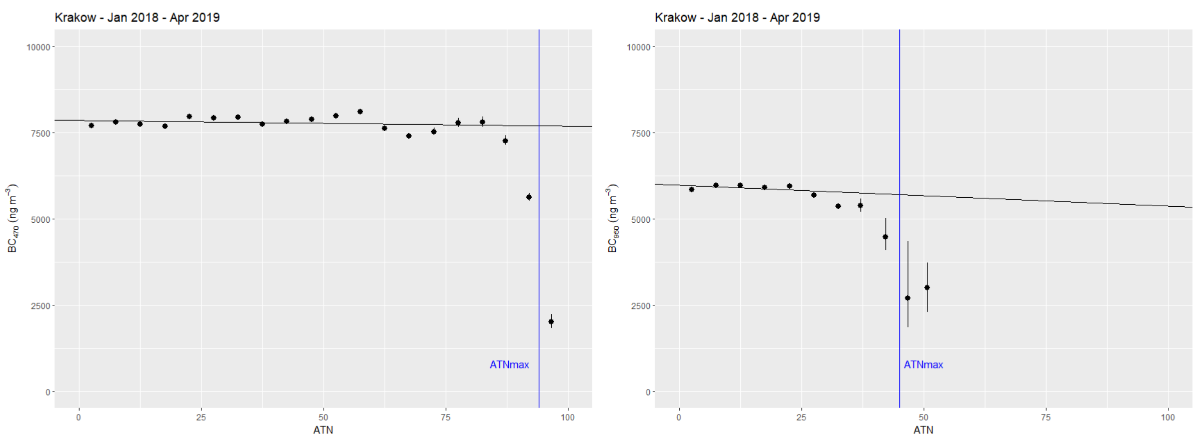

Figure S1. BC(ATN) plots for the measurements at 470 nm (left) and 950 nm (right). The negligible slope demonstrates an absence of loading effects.

Source apportionment uses source specific values of the Ångström exponent (AAE). The traffic features the AAE value between 0.9 and 1.1. The value for solid fuel is less well determined as it depends on the efficiency of combustion. These source specific values are supposed to be representative for the source, but are in fact a single value representing the center of a distribution for this particular source. In the absence of validation measurements (for example C14, Zotter et al., 2017), plotting the probability density function can serve as a guide for the determination of these values as seen in Fig. S2. Source specific values for traffic AAE_{tr} = 0.85 and solid fuel AAE_{sf}= 1.9 were selected.

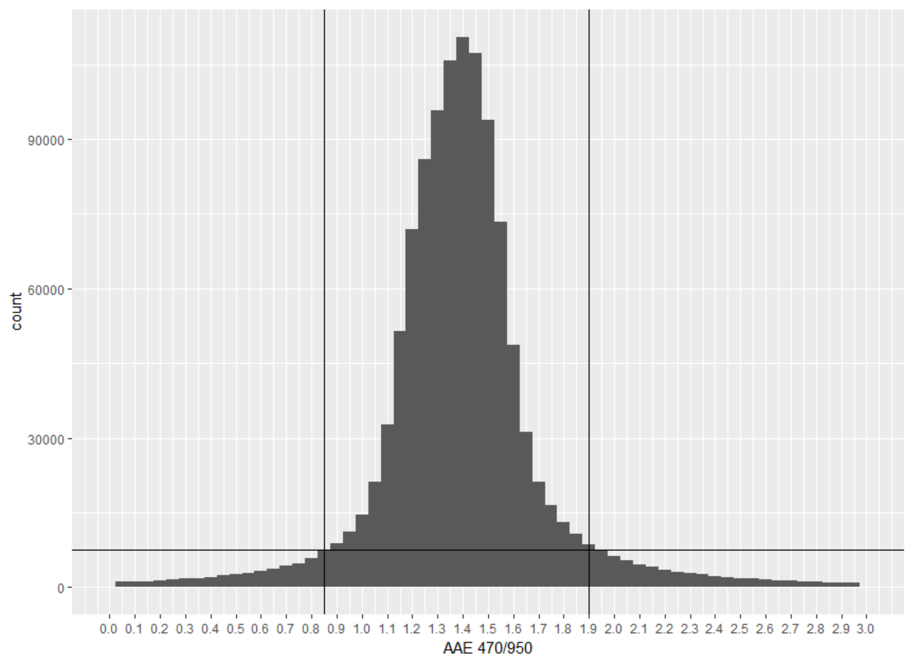

Figure S2. The absorption Ångström exponent (AAE) probability density function.

S2 Further supporting material

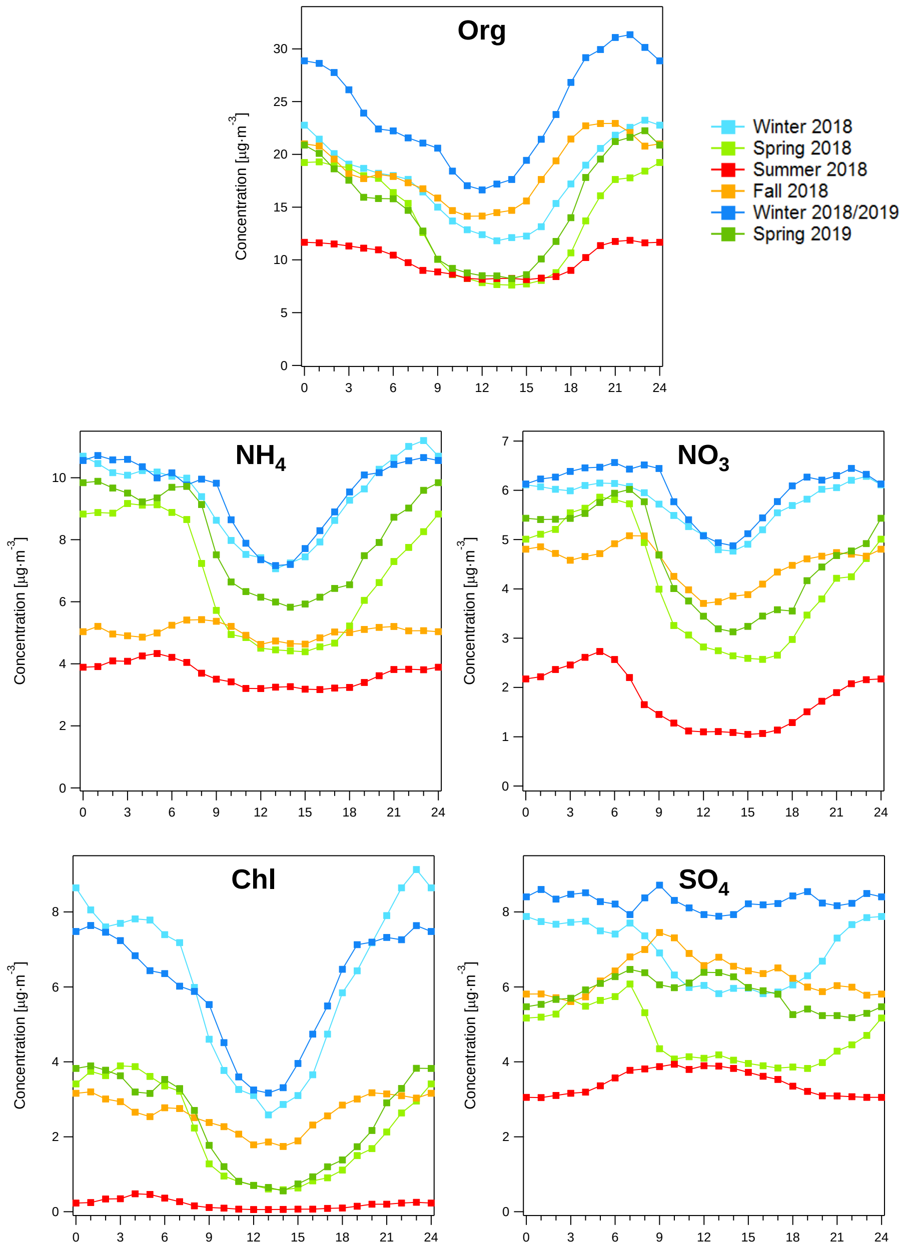

Figure S3. Seasonal diurnal cycles of the ACSM species color-coded by season.

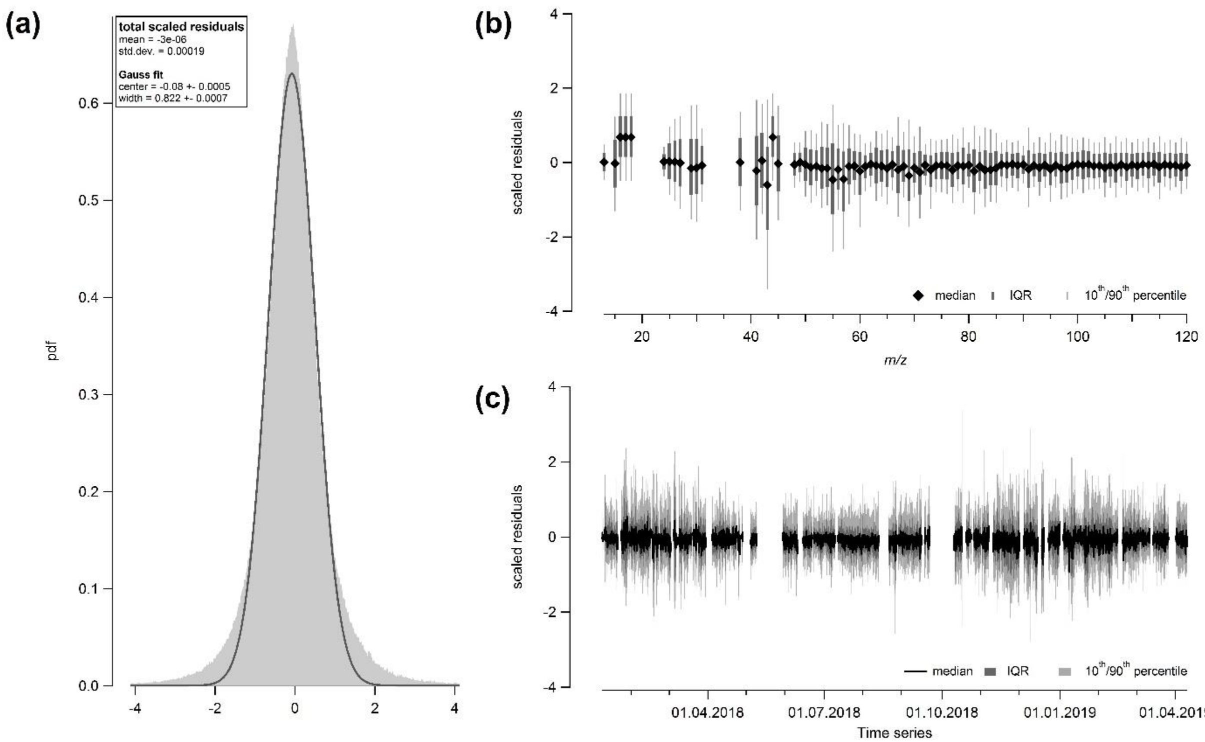

Figure S4. Analysis of the scaled residuals shows no systematic over- or underestimation for (a) the total scaled residuals, (b) the scaled residuals over the *m/z*'s and (c) the scaled residuals over time.

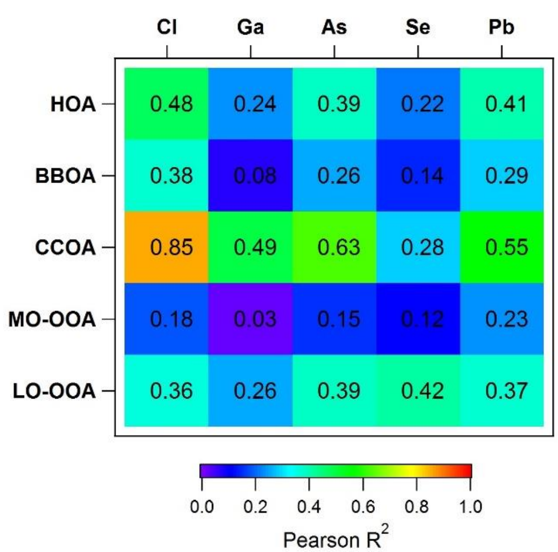

Figure S5. Correlation (Pearson R^2) of the coal-related elements measured by the Xact and all OA factors.

Table S1. Average seasonal OA to eBC ratios.

	2018				2019	
Season	Winter	Spring	Summer	Fall	Winter	Spring
Average OA/eBC (± standard deviation)	2.67 ± 1.03	4.43 ± 2.35	8.22 ± 3.57	5.74 ± 2.33	5.78 ± 2.28	6.01 ± 2.51

References

Drinovec, L., Močnik, G., Zotter, P., Prevot, A. S. H., Ruckstuhl, C., Coz, E., Rupakheti, M., Sciare, J., Muller, T., Wiedensohler, A., and Hansen, A. D. A.: The "dual-spot" Aethalometer: an improved measurement of aerosol black carbon with real-time loading compensation, Atmos. Meas. Tech., 8, 1965-1979, https://doi.org/10.5194/amt-8-1965-2015, 2015.

Drinovec, L., Gregorič, A., Zotter, P., Wolf, R., Bruns, E. A., Prévôt, A. S. H., Petit, J. E., Favez, O., Sciare, J., Arnold, I. J., Chakrabarty, R. K., Moosmüller, H., Filep, A., and Močnik, G.: The filter-loading effect by ambient aerosols in filter absorption photometers depends on the coating of the sampled particles, Atmos. Meas. Tech., 10, 1043-1059, https://doi.org/10.5194/amt-10-1043-2017, 2017.

Gundel, L. A., Dod, R. L., Rosen, H., and Novakov, T.: The relationship between optical attenuation and black carbon concentration for ambient and source particles, Sci. Total Environ., 36, 197–202, , https://doi.org/10.1016/0048-9697(84)90266-3, 1984.

Yus-Díez, J., Bernardoni, V., Močnik, G., Alastuey, A., Ciniglia, D., Ivančič, M., Querol, X., Perez, N., Reche, C., Rigler, M., Vecchi, R., Valentini, S., and Pandolfi, M.: Determination of the multiple-scattering correction factor and its cross-sensitivity to scattering and wavelength dependence for different AE33 Aethalometer filter tapes: A multi-instrumental approach, Atmos. Meas. Tech. Discuss., https://doi.org/10.5194/amt-2021-46, 2021.

Zanatta, M., Gysel, M., Bukowiecki, N., Müller, T., Weingartner, E., Areskoug, H., Fiebig, M., Yttri, K. E., Mihalopoulos, N., Kouvarakis, G., Beddows, D., Harrison, R. M., Cavalli, F., Putaud, J. P., Spindler, G., Wiedensohler, A., Alastuey, A., Pandolfi, M., Sellegri, K., Swietlicki, E., Jaffrezo, J. L., Baltensperger, U., and Laj, P.: A european aerosol phenomenology-5: Climatology of black carbon optical properties at 9 regional background sites across Europe, Atmos. Environ., 145, 346–364, https://doi.org/10.1016/j.atmosenv.2016.09.035, 2016.

Zotter, P., Herich, H., Gysel, M., El-Haddad, I., Zhang, Y. L., Mocnik, G., Huglin, C., Baltensperger, U., Szidat, S., and Prevot, A. H.: Evaluation of the absorption Angstrom exponents for traffic and wood burning in the Aethalometer-based source apportionment using radiocarbon measurements of ambient aerosol, Atmos. Chem. Phys., 17, 4229-4249, https://doi.org/10.5194/acp-17-4229-2017, 2017.